

# The metal nature effects in cryopolymerized metalated poly-*p*-xylylene

L. Alexandrova<sup>a,\*</sup>, E. Sansores<sup>a</sup>, E. Martinez<sup>a</sup>, E. Espinoza Rodriguez<sup>a</sup>, G. Gerasimov<sup>b</sup>

<sup>a</sup>*Departamento de Polimeros, Instituto de Investigaciones en Materiales, UNAM, Circuito Exterior s/n, Ciudad Universitaria, Mexico DF, 04510 Apdo. Postal 70-360, Mexico*

<sup>b</sup>*Karpov Institute of Physical Chemistry, Voronzovo pole 10, Moscow 103064, Russia*

Received 9 November 1999; received in revised form 21 February 2000; accepted 3 March 2000

## Abstract

Ag-, Mg- and Mn-containing poly-*p*-xylylenes were obtained by solid-state photopolymerization of metal-*p*-xylylene mixtures at 77 K. Interaction of the metals with *p*-xylylene before and after its polymerization was studied using IR and UV–Vis spectroscopies. It was shown that Mg and Mn form strongly optically absorbing complexes with *p*-xylylene during codeposition, whereas Ag produces nanoclusters without chemical interaction with monomer and these clusters remain in the polymer matrix practically unchanged.

Mg forms ionic complexes with a large contribution of covalent bonding. The *p*-xylylene in such complexes exists in the form close to its benzenoid one. During polymerization the complexes transform into  $\sigma$ -bonded organomagnesium compounds incorporated within the polymer chains.

Mn as a transition metal produces complexes of two types. Complexes of the first type are similar to those of Mg demonstrating similar behavior in course of polymerization, whereas those of the second type, formed by the interaction of d-orbitals of Mn with  $\pi$ -orbitals of *p*-xylylene, are destroyed during polymerization. © 2000 Published by Elsevier Science Ltd.

**Keywords:** Metal–polymer systems; Poly-*p*-xylylene; Metal clusters

## 1. Introduction

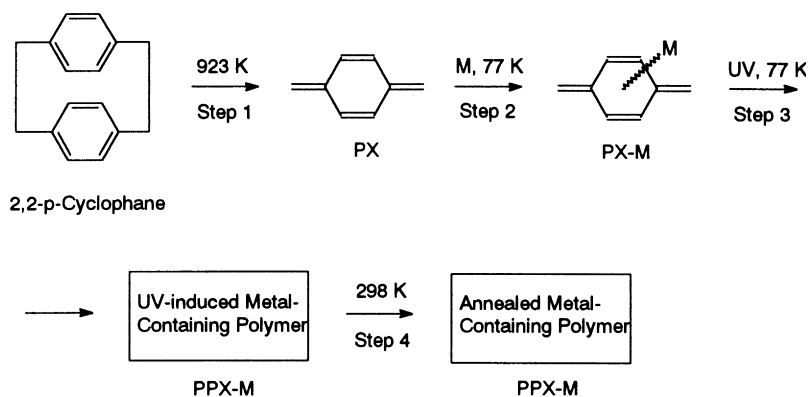
Metal-containing polymers belong to a challenging, intensively developing field of modern material science because of the already existing and potential applications of these materials in opto-electronics, chemical and biochemical catalysis [1–6]. Metal centers within a polymeric matrix can provide a variety of structures such as metal complexes immobilized on a solid support or nanoparticles, which are nowadays of special interest [2,3]. Nanoscale metal clusters are not only at the interface of atomized and solid materials but also exhibit their own specific features [7,8]. The variety of useful physical and chemical properties, including high catalytic activity, magnetism, nonlinear optical effects, etc. depend crucially on the cluster size [3,8]. The main tasks in the preparation of such materials are size control and elimination of cluster coagulation and these may be achieved by high viscosity of polymers

Different strategies are used to fabricate polymer–metal systems, such as treatment of polymers with metal vapors

[9], plasma polymerization in conjunction with metal deposition [10] and free radical polymerization of variously prepared monomer–metal mixtures [3,11].

For our investigations the Gorham process of producing poly-*p*-xylylenes (PPX) was chosen (Scheme 1). This involves the vacuum pyrolysis of *p*-xylylene cyclic dimer, [2.2]-*p*-cyclophane, to afford an extremely reactive monomer of *p*-xylylene (PX) in 100% yield. The vapor deposition of the latter on a substrate leads to a polymeric coating at room or lower temperatures [12]. The technology of this process, because of its high selectivity, makes it very attractive to be combined with metal vapor deposition. Moreover, PX, because of its high reactivity, could be polymerized quantitatively under UV-irradiation even in the solid state at liquid nitrogen temperature giving a fairly high molecular weight polymer with a structure close to  $\beta$ -modification of PPX [13]. This allowed us not only to obtain, but also to polymerize metal–PX mixtures directly at cryogenic temperatures without heating. Under such conditions, when the thermal movement of the molecules is frozen, the initial metal clusters or organometallic assemblies generated during cryosynthesis of the metal–monomer mixtures should be fixed in the obtained polymeric matrix. Thus, low temperature formation followed by

\* Corresponding author. Tel.: + 52-5-622-4582; fax: + 52-5-616-120.  
E-mail address: laz@servidor.unam.mx (L. Alexandrova).



Scheme 1.

photopolymerization of the solid metal–PX mixture could give new metastable structures, which cannot be obtained by other methods.

In a series of previous publications we have demonstrated that different metal species can be readily incorporated into the cryopolymerized PPX matrix in the form of various structures and nanoclusters with the composition being strongly dependent on the nature of metal introduced [14–16]. Only limited data is available on how different metals interact with the polymeric matrix, therefore in this work we have carried out spectral analysis of the speciation of silver, magnesium and manganese within the PPX matrix. A comparative study of the polymerization of PX in the presence of these metals has shown that Mg and Mn form strongly optically absorbing intermediates on interaction with PX prior to polymerization, whereas this is not true for Ag, which produces clusters without chemical interaction with PX and these cluster assemblies remain in the polymer matrix.

## 2. Experimental

The technology of preparation of the poly-*p*-xylylene–metal (PPX–M) films is demonstrated in Scheme 1. The PX was produced by gas-phase pyrolysis of [2.2]-*p*-cyclophane (Aldrich) in vacuum (Gorham method). The solid *p*-cyclophane was sublimated at 383 K and the vapors were passed through a pyrolytic quartz tube at 923 K. Spectral measurements showed that [2.2]-*p*-cyclophane converts into PX without formation of detectable side products under these conditions [12,13]. In the outlet of the pyrolytic tube the PX vapors were mixed with metal (M = Mg, Mn or Ag) vapors produced by sublimation of the corresponding metal at 700 and 1300 K depending on the metal. The PX–M gaseous mixture was deposited onto substrates of quartz or KRS-5 fastened to the steel cell of an optical cryostat, which was cooled to 77 K. The cryostat construction has been reported in detail elsewhere [13,16]. Polymerization of the PX–M mixtures was carried out without extra heating at 77 K using the irradiation from a high-pressure mercury

lamp. The polymerization was monitored by infrared (IR) and UV–Vis spectroscopies at 77 K. The polymerization was considered complete after the disappearance of the monomer bands and the increase of the polymer bands (for details see Section 3). Thickness of the deposited films was measured after polymerization and annealing at ambient temperature using a laser interferometer. The films were between 1 and 3  $\mu\text{m}$  thick. Samples for X-ray and microscopy analysis were separated from the substrate under water, except for Mg-containing ones, which were separated in air.

The IR spectra before and after irradiation were recorded using a Perkin–Elmer 580 spectrophotometer. The UV–Vis spectra were measured on a Shimadzu 365 instrument.

Structural investigation of the films was performed by means of X-ray diffraction (XRD) using a Siemens D5000 diffractometer in transmission mode with  $\text{CuK}\alpha$  radiation. X-ray diffractogram peaks of Cu foil were used as a standard.

Particle-size distribution of the metals incorporated in the polymer matrix was measured on a JEOL JEM-1200 transmission electron microscope (TEM) by counting several hundreds of particles on the electron micrographs and obtaining average diameters.

The amount of metal in the films was evaluated by different routines depending on the metal as described below.

The relative molar Mg content in the polymerized films was estimated from the Mg–O absorbance band at  $450 \text{ cm}^{-1}$  after an oxidation of the Mg in air. Specially prepared mixtures of PPX and MgO were used for calibration [14].

The molar fraction of Mn was measured by atomic absorption spectroscopy. Polymerized films of known weights were burned in  $\text{O}_2$  and the residual solid material was treated with a predetermined quantity of aqueous HCl to dissolve the manganese oxide. The amount of Mn(II) in vapors of the solution was spectrophotometrically measured at 279.5 nm using a Perkin–Elmer 503 spectrometer as described previously [15].

The volume fraction of Ag was estimated from the density of the polymerized film measured by the standard

Table 1

Spectral characteristics of Ag nanocrystals in the solid systems ( $\lambda_{\max}$  and  $\Delta_{1/2}$ , position of the maximum and width at half-maximum of the characteristic absorption band of Ag-nanocrystals;  $D$ , optical density of this band;  $X_{\text{Ag}}^{\text{cr}}$ , molar fraction of Ag nanocrystals)

System	$\lambda_{\max}$ (nm)	$\Delta_{1/2}$ (nm)	$D$ (at $\lambda_{\max}$ )	$X_{\text{Ag}}^{\text{cr}}$ (%)
PX–Ag at 77 K	430	93	0.24	4.2
PPX–Ag at 77 K	430	93	0.25	4.2
PPX–Ag at 298 K	435	96	0.28	5.0
PPX–Ag at 320 K	443	98	1.10	16.3
PPX–Ag at 373 K	443	98	1.22	18.0

flotation method with an accuracy of 5%, and then recalculated into the molar fraction as done elsewhere [16].

The verification of the thus calculated metal concentrations by X-ray fluorescent analysis for several samples showed satisfactory precision. The concentration of the metals in the different samples was in the range 10–20 mol% for Ag- and Mn- and 15–40 mol% for Mg-containing samples.

The thermal stability of the samples was measured in nitrogen atmosphere with the help of a T.A. Instruments, thermogravimetric analyzer TGA 2950 at a heating rate of 10°C/min.

### 3. Results and discussion

#### 3.1. General

The PX monomer generated by the solvent-free vacuum pyrolysis of [2.2]-*p*-cyclophane (Step 1 in Scheme 1) was mixed with a metal vapor and the mixture condensed onto substrate at 77 K. The so obtained PX–M films were colored as in contrast to the colorless pure PX films. The Ag and Mg co-condensates were from yellow to brown, whereas the PX–Mn co-condensates were violet, the color deepness depended on the metal content in the sample. Steps 2 and 3 in Scheme 1 are separated if the cryogenic technique is applied, and this allows one to study independently the UV–Vis and IR spectra of the metal-complexed monomer (PX–M) (the wavy line in Scheme 1 indicates that the binding mode of M is not specified), as well as the changes during conversion of PX–M into metal-containing polymers (PPX–M).

It may be concluded from the spectral data that PX does not polymerize on co-condensation with any of these metals. In fact, the characteristic absorption bands of the quinonoid PX at 470, 870 and 1590  $\text{cm}^{-1}$  were observed in all spectra of the PX–M mixtures, while the typical absorption bands of the polymeric form were absent [13]. However, the nature of the metal manifests itself in the spectra of the original mixtures and also after their photopolymerization. Therefore, it is convenient to consider these independently in the three cases, viz. for Mg, Mn and Ag.

#### 3.2. Spectral and structural features of PX–M and PPX–M

##### 3.2.1. Silver

The IR spectra of Ag-containing monomer films were similar to those of pure monomer films, although about 20% of Ag with respect to PX was introduced. New bands were not detected in the range 400–4000  $\text{cm}^{-1}$ , and hence, co-condensation of PX with Ag did not lead to complexation or the formation of any organometallic compounds. However, in the UV–Vis spectrum of PX–Ag a new band of relatively low intensity with absorption maximum near 430 nm was noticed along with the monomer band at 310 nm. The co-condensation of chloro- and cyano-substituted *p*-xylylenes with Ag under analogous conditions has led to very similar UV–Vis spectra [16,17]. Based on these and related data [18], this absorption was assigned to Ag nanocrystals formed in the PX matrix in the course of the co-deposition at 77 K. Under UV irradiation at 77 K the PX bands disappear completely giving rise to those from PPX; both in the IR and UV–Vis spectra. However, none of spectral characteristics of the 430 nm band, viz. intensity ( $D$ ), maximum position ( $\lambda_{\max}$ ), and half-width ( $\Delta_{1/2}$ ), change in the course of photopolymerization (Table 1). Thus, it can be concluded that the state and amount of Ag nanocrystals were not affected by the cryopolymerization. The annealing of the formed PPX–Ag at 298 K does not result in any significant increase of this band intensity, in contrast to the nanocrystals in the poly-chloro-*p*-xylylene matrix, where about 70% of the introduced Ag were aggregated in such crystals at this temperature [16]. A sharp increase in the absorption at 430 nm was observed only at temperatures 315–320 K. After prolonged storage of the system at these temperatures, further annealing at 373 K changed insignificantly the optical density at 430 nm. Thus, by analogy with the chloro-*p*-xylylene–Ag system it may be concluded that Ag nanocrystals are formed because of agglomeration of Ag nanoparticles of much smaller size (nanoclusters) in the course of annealing. It is known [9,18], that these Ag nanoclusters absorb below 300 nm where their absorption bands overlap with those of PX and PPX, and this is why we failed to identify the presence of the nanoclusters. Assuming that all of the Ag introduced into the PPX matrix exists as the nanocrystals after annealing at 373 K, the value of  $D$  (Table 1) was used to estimate that about 80% Ag in the matrix is in the form of smaller nanoclusters, up to 315 K. Since at a low volume fraction of Ag nanocrystals, their diameter is inversely proportional of  $\Delta_{1/2}$  [19], it can be concluded that the size of the nanocrystals in the PPX matrix remains constant during the photopolymerization and annealing, only their fraction increases. It should also be noted that the solid polymer matrix prevents aggregation of nanoclusters into bigger nanocrystals even at ambient temperature, while if similar Ag clusters are introduced into liquid oligomer or polymer solution they do aggregate readily, but do not form as large conglomerates as in solutions of low molecular weight liquids [9]. The aggregation

Table 2

Selected IR data of PX–Mg system, obtained at 77 K, before and after (PPX–Mg) irradiation (the bands that refer to the metal complexes are shown in bold font)

PX–Mg	PPX–Mg	PX–Mn	PPX–Mn	Attributions <sup>a</sup>
	<b>420</b> w-m			$\nu(\text{Mg}-\text{C})$
470 s		470 s		$\gamma(\text{C}-\text{C quin.})$
<b>740</b> s	<b>740</b> s	<b>740</b> w	<b>740</b> w	$r(\text{CH}_2)$
870 s		870 s		$\gamma(\text{C}-\text{H quin.})$
		<b>1160</b> m-s		$\delta(\text{C}-\text{C} + \text{C}-\text{H quin.})$
<b>1210</b> s	<b>1210</b> s	<b>1210</b> m	<b>1230</b> m	$\nu(\text{CH}_2-\text{C}_6\text{H}_4)$
<b>1485</b> vs	<b>1495</b> vs	<b>1480</b> m	<b>1490</b> m	$\nu(\text{C}-\text{C ring})$
	1510 m		1510 s	$\nu(\text{C}-\text{C benz.})$
		<b>1570</b> s		$\nu(\text{C}-\text{C quin.})$
1590 m		1590 sh		$\nu(\text{C}-\text{C quin.})$
	<b>1605</b> w			$\nu(\text{C}-\text{C benz.})$

<sup>a</sup>  $\nu$ , stretching;  $\delta$ , in-plane deformation;  $\gamma$ , out-of-plane deformation;  $r$ , rocking vibrations.

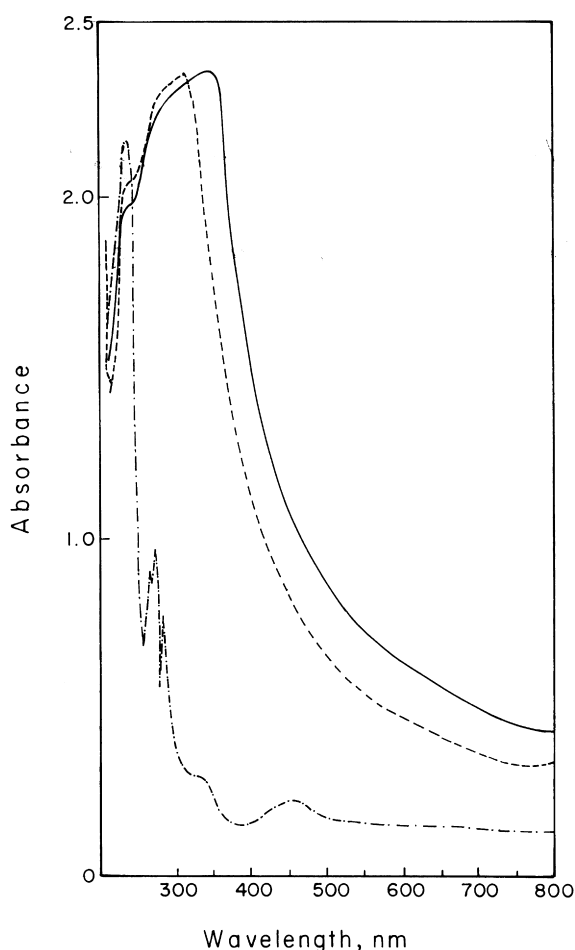


Fig. 1. The UV–Vis spectra of the PX–Mg films with a Mg concentration of about 30 mol%. Solid line, original co-condensate at 77 K; dashed line, after UV irradiation at 77 K (complete polymerization); dot-dashed line, after 36 h of storage at room temperature in vacuum.

of Ag in poly-chloro-*p*-xylylene could occur at lower temperatures than in PPX because in this case the polymerization is incomplete at 77 K; the monomer band at 310 nm was still seen after photopolymerization. There are other data that show a lower reactivity of Cl-substituted PX toward cryogenic photopolymerization compared to unsubstituted PX [20].

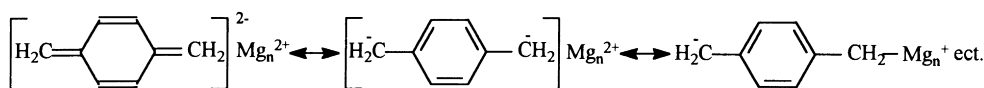
The X-ray diffractogram of the annealed film confirmed the existence of Ag islands with  $d$  spacings  $2.36 \pm 0.02$ ,  $2.08 \pm 0.02$ ,  $1.44 \pm 0.02$  and  $1.23 \pm 0.02$  Å. These values practically coincide with the (111), (200), (220) and (311) reflections of metallic Ag. Very similar characteristics were obtained for the chloro-*p*-xylylene–Ag system, for which a diameter of the nanocrystals of 50 Å was calculated from the half-width of the (111) reflection using the Scherrer equation [16]. Data from our system gave a very similar value of 60 Å, but because of the very low intensity of the peaks the calculation was only of moderate precision.

### 3.2.2. Magnesium

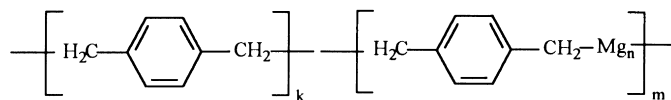
In marked contrast to silver, the loading of Mg into PX at 77 K produces substantial changes both in the UV–Vis and IR spectra, indicative of a chemical interaction between PX and Mg. The most drastic variations in the IR spectra are observed in the range  $500\text{--}1600\text{ cm}^{-1}$ . In addition to characteristic bands of the quinonoid PX at 1595, 870 and  $470\text{ cm}^{-1}$ , there are distinct new bands at 1485 (vs), 1200 (s) and  $750\text{ (s) cm}^{-1}$  (Table 2). Their relative intensity depends on the total amount of Mg introduced (10–40%). It should also be mentioned that there appeared poorly resolved bands in the region of the  $\text{sp}^3$  C–H stretching vibrations between  $2950$  and  $2800\text{ cm}^{-1}$ , whereas the pure PX has only two C–H stretching bands at 3090 and  $3020\text{ cm}^{-1}$  typical of  $\text{sp}^2$  C–H bonds. Thus, the changes in the IR spectra verify the interaction of PX with Mg and show that the PX in this mixture has significant benzenoid character. The most intense band at  $1485\text{ cm}^{-1}$  is of particular interest. Such bands are observed in the spectra of electron-rich benzene derivatives with strong electron-donating substituents when the negative charge is concentrated mostly on the benzene ring [21,22]. In our case the band may be indicative of a notable charge transfer from Mg to PX in the complex. It is important to note that there are no absorption bands of Mg–C stretching vibrations usually observed in interval between  $550$  and  $400\text{ cm}^{-1}$  [23]. This rules out the formation of the  $\sigma\text{-Mg}-\text{C}$  bonds as fragments of  $[-\text{Mg}-\text{CH}_2\text{C}_6\text{H}_4-]$  blocks.

The UV–Vis spectrum of the original PX–Mg co-condensate shows a very intense broad absorbance band with maximum at 345 nm. It masks the bands from the monomer and only residual monomer absorption is seen as a shoulder below 300 nm (Fig. 1). As is known [24,25] organomagnesium compounds such as dibenzylmagnesium and various alkyl derivatives of diphenylmethylmagnesium have absorption maxima at 270–300 nm because of the appreciable degree of covalent character of the Mg–C

bond in these compounds. This differs significantly for the alkali (Na, Li) or alkaline earth (Ca) derivatives, the M–C bonds of which are purely ionic and their absorption maxima lie between 420 and 470 nm. [24]. Since the maximum of the PX–Mg co-condensate is markedly shifted to higher wavelengths, the formation of the covalent structures does not seem plausible. However, the band at 345 nm cannot be considered as an example of a pure charge-transfer band which are usually manifested in the visible region [24]. The formation of neither purely ionic nor covalent structure between such an electron-rich compound as anthracene and Mg was confirmed by  $^1\text{H}$  and  $^{13}\text{C}$  NMR data [26]. The anthracene–Mg complex was interpreted as forming an ion pair with strong interaction between the Mg and the carbon atoms at 9 and 10 positions of anthracene. Theoretical simulations at the AM1 level using MOPAC code [27] show that after a complete geometry optimization the PX molecule with negative charge ( $-2$ ) is quite stable (no negative frequencies were found) and negative charges are mostly concentrated on the carbons of the  $\text{CH}_2$ -groups, with these becoming significantly  $\text{sp}^3$  in character. This benzenoid form of the PX molecule is probably stabilized by interacting with the metal center. Taking this into consideration, together with the IR and UV–Vis data, it may be assumed that the PX–Mg complexes obtained on co-condensation could be rationalized as moderately ionic species involving strong contacts between the metal and the  $\text{CH}_2$  carbons.



Irradiation of the system at 77 K by UV light leads to complete disappearance of the monomer bands at 470, 870 and  $3090\text{ cm}^{-1}$  and the growth of polymeric bands at  $1510$ ,  $2850$  and  $2920\text{ cm}^{-1}$  together with a new band at  $420\text{ cm}^{-1}$  which can be assigned to the Mg–C stretching vibrations (Table 2). The bands ascribed to PX–Mg complexes remain without significant changes and there is only a small shift of the band at  $1485\text{ cm}^{-1}$  to higher frequencies (Table 2). At the same time the position of the UV band moves from 345 to 310 nm (Fig. 1), this is much closer to the absorbance position of organomagnesium compounds with Mg–C  $\sigma$  bonds mentioned above. Therefore we suggest that on polymerization the PX–Mg complexes transform into covalently bound organomagnesium compounds of the type  $[-\text{CH}_2-\text{C}_6\text{H}_4-\text{CH}_2-\text{Mg}_n-]$  where  $\text{Mg}_n$  is a magnesium atom or cluster. These organomagnesium units are incorporated into the polymer chains and form part of a polymer with the structure



The existence of the new band at  $1605\text{ cm}^{-1}$  in the IR spectrum of the polymerized PX–Mg co-condensate is of importance. Such a band is typical for *para*-disubstituted benzenes with the substituents having different Hammett constants [22] ( $-\text{CH}_2-\text{CH}_2-$  and  $-\text{CH}_2-\text{Mg}$  in the present case). Shift of the  $1485\text{ cm}^{-1}$  band to higher frequencies may be explained by a weakening of the metal influence on the benzene ring vibrations in the structure with covalent Mg–C bonds, in comparison to the original PX–Mg complexes in which the Mg interacts with the  $\pi$ -electrons of benzene directly.

Prolonged storage of the cryogenically polymerized system under vacuum at ambient temperature (30–36 h) resulted in the cleavage of the Mg–C bond in the polymer: all of the bands related to the PX–Mg compounds in IR and UV–Vis spectra disappear. The IR spectrum of the annealed system becomes identical to that of pure PPX [14]. The collapse of the  $1495\text{ cm}^{-1}$  band is accompanied by an increase in the benzene ring absorption at  $1510\text{ cm}^{-1}$  and this confirms that the former band corresponds to the benzene ring vibrations in the PX–Mg complexes and PPX–Mg. In the UV–Vis spectrum of the annealed PPX–Mg along with polymeric bands two new weak bands with maxima at 345 and 440 nm are observed. After destruction of the polymer–Mg chemical bonds Mg should obviously be present in the polymer matrix in the form of particles. These two bands in the UV–Vis spectrum suggest the formation of  $\text{Mg}_3$  clusters after annealing, Mg-clusters of

larger size absorb at short wave region and could not be observed because of PPX absorption there [28]. Exposure of the polymeric films to air results in oxidation of Mg and the observation of a characteristic wide band of Mg–O stretching vibrations with maximum at  $460\text{ cm}^{-1}$  on the background of the PPX spectrum [14]. The XRD data also confirmed the oxidation of Mg in the films. The *d*-spacing values of  $2.11 \pm 0.01$ ,  $1.48 \pm 0.02$  and  $0.93 \pm 0.02\text{ \AA}$  which correspond to the (200), (220) and (420) reflections of MgO, respectively, were seen on the diffractogram. The reflections of metallic Mg were not observed. The cluster size calculated from the half-width of the (200) reflection gave a value approximately  $35\text{ \AA}$ .

### 3.2.3. Manganese

In general, the behavior of the Mn system is closer to the Mg one than to the Ag case. The spectral data obtained demonstrate that Mn also forms complexes with PX.

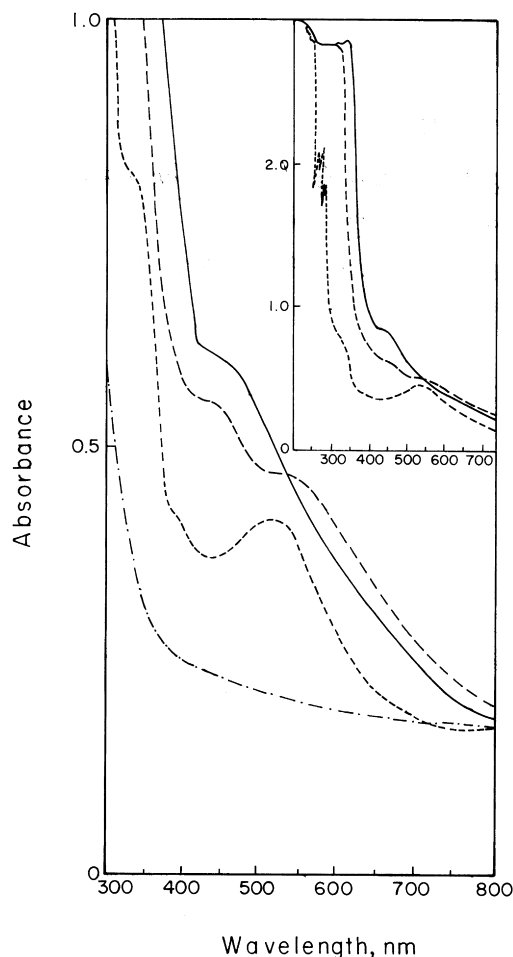


Fig. 2. The UV-Vis spectra of the PX-Mn films with a Mn concentration of about 20 mol%. Solid line, original co-condensate at 77 K; dashed line, after 1 h of UV irradiation at 77 K (incomplete polymerization); dotted line, after 2.5 h of UV irradiation at 77 K (complete polymerization); dot-dashed line, after 12 h of storage at room temperature in vacuum.

However, in contrast to Mg, there are two sets of new IR bands whose behavior differs in the course of UV irradiation. The first set is comprised of the 1160 and 1570  $\text{cm}^{-1}$  bands which disappear on irradiation, whereas the second one (740, 1210 and 1480  $\text{cm}^{-1}$ ) remains unchanged (Table 2). The positions of the second set bands coincide with those of the spectrum of the PX-Mg co-condensate but their relative intensity is much lower in the Mn case at comparable metal concentrations. It was noted that, in contrast to other transition metals, Mn forms primarily ionic complexes with some unsaturated hydrocarbons, the IR spectra of which are similar to those of Mg compounds [29,30]. Therefore the bands of the second set can be assigned to similar rather ionic structure  $\text{Mn}^{2+}\text{PX}^{2-}$  as was done for the Mg-PX system. It should be mentioned that the first set of bands (at 1570 and 1160  $\text{cm}^{-1}$ ) predominate in intensity over those of the second: at low Mn content (less than 10%) only these two bands and those of the pure PX are clearly seen in the spectrum. Manganese, distinct from magnesium, is a transition metal and may form  $\pi$ -complexes involving

its d-orbitals and the  $\pi$ -orbitals of PX, presumably with a 1:1 and 2:1 ligand-to-metal composition. The band at 1570  $\text{cm}^{-1}$  is then most likely related to the skeletal in-plane vibrations of the quinonoid ring in these  $\pi$ -complexes, with this shifted to a lower frequency region compared to the analogous band of free PX (1590  $\text{cm}^{-1}$ ) [31]. The band at 1160  $\text{cm}^{-1}$  can be assigned to deformational vibrations of the quinonoid ring, including skeletal and C-H bond vibrations, and this becomes much more pronounced in the PX-Mn  $\pi$ -complexes in comparison to the free PX [15].

Such  $\pi$ -complexes of Mn with quinonoid PX molecules should obviously be destroyed during polymerization with the conversion of the quinonoid PX into its benzenoid form. However, these complexes do not rearrange into the ionic species (similar to the Mg case), or any other structures, nor is the Mn liberated from them incorporated into the polymer chains. This is because no new bands, nor an increase in the intensity of the other bands, except those typical of PPX, were observed in the IR spectrum after irradiation.

The complexation, however, stabilizes the PX molecules and normally irradiation times of two to three times longer were needed for polymerization of PX in these complexes (this being indicated by the disappearance of the 1570  $\text{cm}^{-1}$  absorption) as compared to the free PX, for the same intensity of the UV source.

The UV-Vis spectrum of the initial PX-Mn co-condensate shows a very strong absorption in the region between 300 and 350 nm, the character of which is similar in total to the PX-Mg system's spectrum. Unfortunately, because of extremely high intensity we failed to determine its maximum position. On this background a longer-wavelength absorption, with maximum near 420 nm, was also observed (Fig. 2). Irradiation of the co-condensate leads to a shift of the total absorption to a shorter-wavelength region, decreasing of the band intensity at 420 nm and appearance of a new absorption in the region 510–520 nm (Fig. 2). This, together with the IR data discussed above, allows us to assume that the absorption around 420 nm is related to the  $\pi$ -complexes. The evolution, during irradiation, of the band at 520 nm is referred to complexes of Mn with polymeric radicals, whose band appears at 320 nm after vanishing of the PX bands at 310 nm (Fig. 3, dotted line) [15].

By analogy with the PX-Mg system we tentatively assume that the ionic PX-Mn complexes transform into  $\sigma$ -bonded organomanganese compounds  $-\text{CH}_2-\text{C}_6\text{H}_4-\text{CH}_2-\text{Mn}_n-$  incorporated into the polymer chains, though the band of Mn-C stretching vibration at 460–480  $\text{cm}^{-1}$  [32] was not identified in the spectrum after photopolymerization, probably, because of both low concentration of such units and low extinction coefficient of this band.

As in the case of the PX-Mg system, prolonged storage at ambient temperature in vacuum (8–12 h) leads to a gradual fading of all bands of the complexes in the IR and UV-Vis spectra leaving the spectra of free PPX. We believe that decomposition of the organomanganese compounds and complexes leads to the formation of Mn clusters.

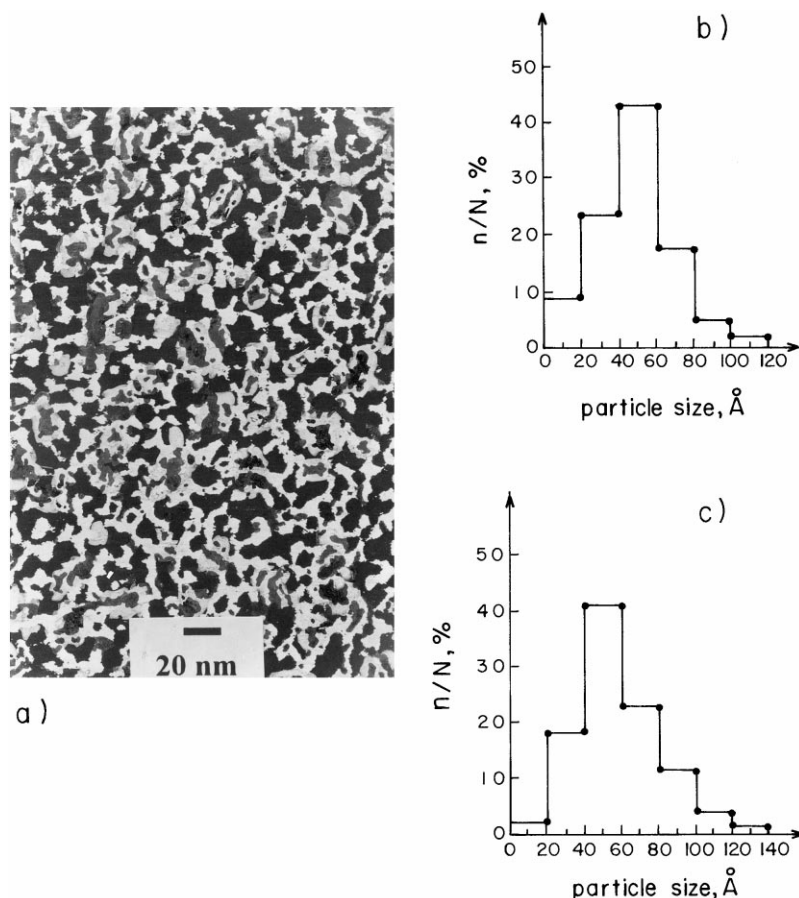


Fig. 3. TEM photographs of: (a) the annealed Ag-PPX and histograms of the size distribution for (b) Ag-PPX and (c) Mn-PPX.

X-ray diffractograms of the Mn-containing films were of very poor quality because of the very low intensity and considerable width of peaks. We managed to measure the position of only one peak with a  $d$ -spacing of  $4.00 \pm 0.03$  Å. This coincides with the (111) reflection of metallic Mn of a form which is intermediate between the  $\alpha$ - and  $\beta$ -Mn [33].

The Ag- and Mn-containing polymers were investigated by TEM. It was found that there were globular particles of sizes between 20 and 120 Å quite homogeneously dispersed within the polymeric matrix. Histograms of the size distribution (Fig. 3) show that the main particle size is between 40 and 60 Å, in good agreement with the calculated values from X-ray data.

The TGA analysis of the Ag- and Mn-filled films did not demonstrate any significant difference in the decomposition process between these and free PPX. The thermal decomposition started at 462°C for Ag- and at 458°C for Mn-containing samples in an inert atmosphere; these temperatures are close to the initial decomposition temperature of ordinary PPX (450°C) [34] measured under the same conditions.

#### 4. Conclusions

The data obtained for all three metals studied have

demonstrated their different ability to interact with PX during co-deposition onto substrates at 77 K, and their distinct behavior during cryopolymerization.

Silver does not show any tendency for interaction and forms nanoclusters during co-deposition which are not affected by cryopolymerization. There is little observable change during annealing of the system up to room temperature. Only annealing at higher temperature leads to aggregation of the nanoclusters into larger nanocrystals.

Magnesium interacts strongly with PX during co-deposition, forming ionic complexes with a large contribution of covalent bonding. PX in such complexes exists in its benzenoid form. During polymerization the complexes transform into  $\sigma$ -bonded organomagnesium compounds incorporated within the polymer chains. Annealing of the PPX-Mg system in vacuum leads to gradual decomposition of the Mg-C bonds in the polymer and Mg is released in the form of clusters within the polymeric matrix.

Manganese also interacts with PX and forms complexes of two kinds that differ in their behavior during cryopolymerization. Complexes of the first type are similar to those of Mg demonstrating similar behavior in the course of polymerization and further annealing. The species of the second type are  $\pi$ -complexes, formed by the interaction of the  $d$ -shell of the Mn with the  $\pi$ -orbitals of the quinonoid PX.

These  $\pi$ -complexes are destroyed by polymerization with the transformation of the quinonoid PX into its benzenoid form.

The TEM analysis of the annealed Ag- and Mn-containing films demonstrated very similar particle sizes and distributions within the polymeric matrix. The most common particle size was between 40 and 60 Å. These films also demonstrated a bit higher thermostability in an inert atmosphere in comparison to free PPX; their thermal decomposition started at temperatures 8–10°C higher than for pure PPX.

### Acknowledgements

The authors gratefully acknowledge the financial support provided by CONACYT grand 27682U. The authors also thank Miguel Angel Canseco for the spectral and TGA measurements, Leticia Baños Lopez for X-ray and Jose Guzman Mendoza for TEM analysis.

### References

- [1] Lewis LN. *Chem Rev* 1993;93(8):2693–730.
- [2] Reetz MT, Wolfgang H, Quaiser SA, Stimming U, Breuer N, Vogel R. *Science* 1995;267(5196):367–71.
- [3] Golden JH, Deng H, DiSalvo FJ, Frechet JMJ, Thompson PM. *Science* 1995;268(5216):1463–6.
- [4] Schmid G. *Chem Rev* 1992;92(8):1709–27.
- [5] Schuhmann W. *Biosens Bioelectron* 1995;10(2):181–6.
- [6] Ryabov AD, Kurova VS, Goral VN, Reshetova MD, Razumiene J, Simkus R, Vaccinaviaus V. *Chem Mater* 1999;11(3):600–4.
- [7] Bonacic-Koutecky VP, Fantucci P, Koutecky J. *Chem Rev* 1991;91(5):1035–105.
- [8] Jornet J. *Z Phys D: Atoms, Molecules and Clusters* 1992;24:247–75.
- [9] Andrews MP, Ozin GA. *Chem Mater* 1989;1(2):174–81.
- [10] Harada M, Asakura K, Toshima N. *J Phys Chem* 1994;98(10):2653–62.
- [11] Gardenas-Triviño G, Camillo RC, Klabunde KJ. *Polym Bull* 1991;25(3):315–8.
- [12] Alexandrova L, Vera-Graziano R. In: Salamone JC, editor. *Polymeric materials encyclopedia*, vol. 9. Boca Raton, FL: CRC Press, 1996. p. 7180–9.
- [13] Alexandrova LN, Shundina LV, Gerasimov GN, Kardash I. *Polym Sci USSR (Trans: Vysokomol Soed) A* 1993;35(4):435–9.
- [14] Alexandrova LN, Sochilin VA, Gerasimov GN, Kardash I. *Polymer* 1997;38(3):721–4.
- [15] Alexandrova L, Likhatchev D, Muhl S, Salcedo R, Gerasimov G, Kardash I. *J Inorg Organometal Polym* 1998;8(3):157–65.
- [16] Gerasimov GN, Sochilin VA, Chvalun SN, Volkova LV, Kardash I. *Macromol Chem Phys* 1996;197(4):1387–93.
- [17] Sochilin VA, Kardash I, Gerasimov GN. *Vysokomol Soed A* 1995;37(12):1938–41.
- [18] Andrews MP, Ozin FA. *J Phys Chem* 1986;90(1):2922–8 (see also p. 2929–2038).
- [19] Charle KP, Frank F, Schulze W. *Ber Bunsenges Phys Chem* 1984;88(4):350–4.
- [20] Alexandrova, LN. Unpublished data.
- [21] Maslowsky E. *Vibrational spectra of organometallic compounds*. New York: Wiley, 1977 (chap. 3).
- [22] English PJJ, Katrizky AR, Tidwell TT, Topson R. *J Am Chem Soc* 1968;90(7):1767–74.
- [23] Ashby ES, Goel AB. *J Org Chem* 1977;42(22):3480–5.
- [24] Arest-Yakubovich AA, Basova RV, Birman EA. *Vysokomolekul Soed B* 1979;21(3):226–9.
- [25] Ebel HF, Wagner BO. *Chem Ber* 1971;104(1):307–19.
- [26] Bogdanovic B, Liao S, Mynott R, Schlichte K, Westeppe U. *Chem Ber* 1984;117(4):1378–92.
- [27] Dewar MJS, Zoebich EG, Healy EF, Stewart JJP. *J Am Chem Soc* 1985;107(13):3902–9.
- [28] Imuzu Y, Klabunde KJ. *Inorg Chem* 1984;23(22):3602–5.
- [29] Wilkinson G, Cotton FA, Birmingham JM. *J Inorg Nucl Chem* 1956;2:95–113.
- [30] Billups WE, Moorehead AW, Ko PJ, Margrave JL, Bell JP, McCormic FB. *Organometallics* 1988;7(10):2230–1.
- [31] Nakamoto K. *Infrared and Raman spectra of inorganic and coordination compounds*. 4th ed.. New York: Wiley, 1986 (chap. 4).
- [32] Sourissean C, Pasquier BJ. *Helv Spectrochim Acta A* 1975;31(4):287–302.
- [33] Lux H, Ignatovicz A. *Chem Ber* 1968;101:2995–7.
- [34] Joesten BL. *J Appl Polym Sci* 1974;18(2):439–48.